On Downlink Beamforming With Greedy User Selection: Performance Analysis and a Simple New Algorithm

Goran Dimić, *Member, IEEE,* and Nicholas D. Sidiropoulos, *Senior Member, IEEE*

***Abstract*—This paper considers the problem of simultaneous multiuser downlink beamforming. The idea is to employ a transmit antenna array to create multiple "beams" directed toward the individual users, and the aim is to increase throughput, measured by sum capacity. In particular, we are interested in the practically important case of more users than transmit antennas, which requires user selection. Optimal solutions to this problem can be prohibitively complex for online implementation at the base station and entail so-called *Dirty Paper* (DP) precoding for known interference. Suboptimal solutions capitalize on multiuser (selection) diversity to achieve a significant fraction of sum capacity at lower complexity cost. We analyze the throughput performance in Rayleigh fading of a suboptimal greedy DP-based scheme proposed by Tu and Blum. We also propose another user-selection method of the same computational complexity based on simple zero-forcing beamforming. Our results indicate that the proposed method attains a significant fraction of sum capacity and throughput of Tu and Blum's scheme and, thus, offers an attractive alternative to DP-based schemes.**

***Index Terms*—Beamforming, downlink, multiuser diversity.**

I. Introduction

TRANSMIT antenna arrays can be utilized in two basic ways or a combination thereof: space-time coding and spatial multiplexing. The former can be used without Channel State Information (CSI) at the transmitter and allows mitigation of fading and exploitation of transmit-receive diversity. However, if CSI is known at the transmitter, higher throughput can be attained using spatial multiplexing, which can be implemented as multibeam transmit beamforming. Until recently, transmit beamforming was mostly considered for voice services in the context of the cellular downlink. With the emergence of third- and fourth-generation (3G and 4G) systems, higher emphasis is being placed on packet data, which are more delay-tolerant but require much higher throughput. Hence, we have the recent interest in transmit beamforming strategies for the cellular downlink that aim to attain the sum capacity of the wireless channel [1], [11], [13]–[16], [18], [19].

The scenario of interest can be modeled as a nondegraded Gaussian broadcast channel (GBC). Let N be the number of antennas at the transmitter [Base Station (BS) in a cellular context], and consider a cluster of M mobile users, each equipped with a single receive antenna. The channel between each transmit and receive antenna is constant over a certain time interval and is known at the BS. The received signal is corrupted by Additive White Gaussian Noise (AWGN) that is independent across users. The BS may transmit simultaneously, using multiple transmit beams, to more than one user in the cluster.

Since the receivers cannot cooperate, successful transmission critically depends on the transmitter's ability to simultaneously send independent signals with as small interference between them as possible. Caire and Shamai [1] proposed a multiplexing technique based on coding for known interference, known as "Writing on Dirty Paper," Costa precoding [2], or dirty paper (DP) coding. In [2], it is proven that in an AWGN channel with additional additive Gaussian interference, which is known at the transmitter in advance (noncausally), it is possible to achieve the same capacity as if there were no interference. Assuming Costa precoding and known channels at the transmitter, Vishwanath *et al.* [14] and Yu and Cioffi [19] have proposed algorithms that evaluate sum capacity of the GBC along with the associated optimal signal covariance matrix. However, both approaches require convex optimization in (order of) MN variables to find the optimal signal covariance matrix. Jindal *et al.* [7] have recently proposed a more efficient iterative algorithm, which requires $O(M^2N^2)$ operations per iteration.

The complexity of the aforementioned optimal strategies can be problematic for online implementation, especially when M is large. A reduced-complexity suboptimal solution to sum rate maximization is proposed in [1]. It suggests the use of QR decomposition of the channel matrix combined with DP coding at the transmitter. The combined approach nulls interference between data streams, and hence, it is named zero-forcing dirty-paper (ZF-DP) precoding. If $N \geq M$, ZF-DP is proven to be asymptotically optimal at both low and high SNR but suboptimal in general, whereas ZF beamforming without DP coding is optimal in the low SNR regime and yields the same slope of

Manuscript received May 12, 2004; revised November 26, 2004. This work was supported in part by the European Research Office (ERO) of the U.S. Army under Contract N62558-03-C-0012 and in part by the Army Research Laboratory under Cooperative Agreement DADD19-01-2-0011. Any opinions, findings and conclusions or recommendations expressed in this material are those of the authors and do not necessarily reflect the views of ERO and ARL of the U.S. Army. U.S.–Greek exchange supported in part by a GSRT collaborative exchange grant. An earlier version of part of this work appears in *Proc. IEEE ICASSP 2004*, May 17-21, 2004, Montréal, QC, Canada. The associate editor coordinating the review of this manuscript and approving it for publication was Dr. Vikram Krishnamurthy.

G. Dimic was with the Department of Electrical and Computer Engineering, University of Minnesota, Minneapolis MN 55455 USA. He is now an independent researcher/consultant in Belgrade, Serbia and Montenegro (e-mail: gorandimic@ieee.org).

N. D. Sidiropoulos is with the Department of Electrical and Computer Engineering, Technical University of Crete, Chania, Crete 73100, Greece (e-mail: nikos@ telecom.tuc.gr).

Digital Object Identifier 10.1109/TSP.2005.855401

throughput versus SNR in decibels as the sum capacity curve at high SNR. For the case of $N \geq M$, Spencer and Haardt [11] considered ZF beamforming without DP coding, and Samardzija and Mandayam [10] compared ZF beamforming with QR-decomposition-based spatial prefiltering coupled with DP coding.

If $N < M$, [1] has shown that random selection of $U \leq N$ users incurs significant throughput loss for both ZF-DP and ZF schemes. Tu and Blum [13] have proposed an algorithm based on ZF-DP, with a greedy user-selection procedure, named greedy ZF-DP (gZF-DP). In [13], it is shown by simulations that the throughput of gZF-DP is a significant fraction of the sum capacity. This is achieved by means of *multiuser diversity*. For the case of $N \leq M$, Viswanathan *et al.* [16] considered the problem of achieving any point in the capacity region and not only maximum sum capacity. They proposed ZF beamforming coupled with a user-selection scheme that schedules N users using an exhaustive search over a set of K_T users with the highest *individual* SINR $(N \leq K_T \leq M)$. The throughput of this scheme was compared to the throughput of a DP-coding-based optimal algorithm, and it was reported that as K_T approaches M, the throughput of ZF with exhaustive user selection comes close to the throughput of the optimal algorithm when each receiver has one antenna [16].

An important shortcoming of DP coding is that it requires vector coding, and depending on the SNR, it may require long temporal block lengths to be well approximated in practice. In particular, the required block length decreases as SNR increases, with a block length of one being adequate at sufficiently high SNR. At low and moderate SNR, a good approximation of DP can be computationally demanding with the current state-of-art [8], [18], [20]. For this reason, we advocate herein a more pragmatic approach, based on plain ZF beamforming.

Our goal is to investigate low-complexity downlink beamforming solutions that come close to attaining sum capacity for the practically important case wherein the number of downlink users (M) is larger than the number of transmit antennas (N), which entails user selection. Our aim is three-fold: i) Analyze gZF-DP to better understand the effects of multiuser diversity; ii) propose a simpler greedy alternative, based on ZF beamforming and dubbed ZFS, which does not use DP coding; and iii) assess the performance of both gZF-DP and ZFS relative to sum capacity. The key idea is that multiuser diversity can largely make up for the use of simple linear processing in lieu of more complex schemes. The performance analysis of gZF-DP is useful in system design, and ZFS is appealing from a practical standpoint. In particular, we will show that the complexity of the selection procedure of the proposed algorithm is the same as that of gZF-DP. Our simulation results indicate that at moderate and high SNR, ZFS has equal slope of throughput versus SNR as the gZF-DP and the capacity curve. It achieves a significant fraction of throughput of the gZF-DP algorithm and remains close to sum capacity for all SNR for a small to moderate number of transmit antennas.

We note that an inherent drawback of the maximum sum capacity criterion is the lack of fairness guarantees, at least in the short run. While this could be compensated over a longer timeline due to channel variations, it remains that certain users may be completely shut off during a scheduling epoch. Whether this is appropriate or not depends on the context; on this issue, see also [1], [11], [13]–[16], [18], and [19].

The rest of the paper is organized as follows. The problem of sum rate maximization is formulated in Section II. This is followed by a review of the gZF-DP algorithm, a description of the proposed ZFS algorithm, and a comparison of the complexities of the two algorithms in Section III. In Section IV, the throughput performance of the gZF-DP algorithm in independent Rayleigh fading is analyzed. Simulation-based comparison of the throughput performances of gZF-DP and ZFS is provided in Section V. Conclusions are drawn in Section VI.

II. Problem Formulation

Let $h_{m,n}$ model the quasistatic, flat-fading channel between transmit antenna n and the receive antenna of user m, and denote $\mathbf{h}_m := [\, h_{m,1} \quad h_{m,2} \quad \ldots \quad h_{m,N} \,]$. Note that $\mathbf{h}_m$ is a row vector. Thus, the channel matrix $\mathbf{H}$ is

$$\mathbf{H} = [\, \mathbf{h}_1^* \quad \mathbf{h}_2^* \quad \ldots \quad \mathbf{h}_M^* \,]^* \tag{1}$$

where $(\cdot)^*$ denotes conjugate-transpose. $\text{rank}(\mathbf{H}) = \min(N, M)$ with probability 1, due to the assumed statistical independence and continuous distribution of the channel vectors. Throughout the paper, we are interested in the case $N < M$ so that we assume that $rank(\mathbf{H}) = N$. Collecting the baseband-equivalent outputs, the received signal vector is

$$\mathbf{x} = \mathbf{H}\mathbf{y} + \mathbf{z} \tag{2}$$

where $\mathbf{y}$ is the transmitted signal vector, and $\mathbf{z}$ is the noise vector. The signal covariance matrix is $\mathbf{C}_y = E[\mathbf{y}\mathbf{y}^H]$. The total transmit power is constrained to P. The sum capacity of such a vector Gaussian broadcast channel is [15]

$$C = \sup_{\mathbf{C}_y \in \mathcal{A}} \log\det(\mathbf{I} + \mathbf{H}\mathbf{C}_y\mathbf{H}^*) \tag{3}$$

where $\boldsymbol{\mathcal{A}}$ is the set of N by N non-negative diagonal matrices $\mathbf{C}_y$ with $\text{Trace}[\mathbf{C}_y] \leq P$.

Using only linear spatial processing at the transmitter, which is a suboptimal strategy, we obtain the following model. Let $\mathbf{w}_m = [w_{1,m} \; w_{2,m} \; \ldots \; w_{N,m}]^T$ ($(\cdot)^T$ denotes transpose) be the beamforming weight vector for user m. The beamforming weight matrix $\mathbf{W}$ is

$$\mathbf{W} = [\mathbf{w}_1 \; \mathbf{w}_2 \; \cdots \; \mathbf{w}_M]. \tag{4}$$

Collecting the baseband-equivalent outputs, the received signal vector is

$$\mathbf{x} = \mathbf{H}\mathbf{W}\mathbf{D}\mathbf{s} + \mathbf{z} \tag{5}$$

where $\mathbf{s}$ is the transmitted signal vector containing uncorrelated unit-power entries, and

$$\mathbf{D} = \begin{bmatrix} \sqrt{p_1} & 0 & \cdots & 0 \\ 0 & \sqrt{p_2} & \cdots & 0 \\ \vdots & \vdots & \ddots & \vdots \\ 0 & 0 & \cdots & \sqrt{p_M} \end{bmatrix} \tag{6}$$

accounts for power loading (the columns of $\mathbf{W}$ are thus normalized to unit norm). Note that the elements of $\mathbf{x}$ are physically distributed across the M mobile terminals. Multiuser decoding is therefore not feasible; hence, each user treats the signals intended for other users as interference. Noise is assumed to be circular complex Gaussian, zero-mean, and uncorrelated with variance of each complex entry $\sigma^2 = 1$.

The desired signal power received by user m is given by $|\mathbf{h}_m \mathbf{w}_m|^2 p_m$. The Signal-to-Interference plus Noise Ratio (SINR) of user m is

$$\mathrm{SINR}_m = \frac{|\mathbf{h}_m \mathbf{w}_m|^2 p_m}{\sum_{i \neq m} |\mathbf{h}_m \mathbf{w}_i|^2 p_i + \sigma^2}. \quad (7)$$

The linear beamforming problem can now be formulated as

$$\boxed{\begin{array}{c}\max_{\mathbf{W},\mathbf{D}} \sum_{m=1}^{M} \log_2(1 + \mathrm{SINR}_m) \\ \text{subject to} \|\mathbf{WD}\|_F^2 \leq P\end{array}} \quad (8)$$

where $\|\cdot\|_F$ denotes Frobenius norm, and P stands for a bound on average transmitted power.

Attaining capacity requires Gaussian signaling and long codes, yet the logarithmic SINR reward can be motivated from other, more practical perspectives as well. It can be shown that it measures the throughput of QAM-modulated systems over both AWGN and Rayleigh fading channels. The intuition is that SINR improvements eventually yield diminishing throughput returns.

III. Reduced-Complexity Algorithms

A. Greedy Zero-Forcing Dirty-Paper Algorithm

In [1], Caire and Shamai have proposed a suboptimal solution to (3) based on the QR-type decomposition [6] of the channel matrix $\mathbf{H} = \mathbf{LQ}$ obtained by applying Gram–Schmidt orthogonalization to the rows of $\mathbf{H}$. $\mathbf{L}$ is a lower triangular matrix, and $\mathbf{Q}$ has orthonormal rows. Setting $\mathbf{W} = \mathbf{Q}^*$, (5) yields a set of interference channels

$$x_m = l_{m,m}\sqrt{p_m} s_m + \sum_{j<m} l_{m,j}\sqrt{p_j} s_j + z_m, \quad m = 1, \ldots, N \quad (9)$$

while no information is sent to users $m = N+1, \ldots, M$. In order to eliminate the interference term $I_m = \sum_{j<m} l_{m,j}\sqrt{p_j} s_j$, the input signals $\sqrt{p_m} s_m$, for $m = 1, \ldots, N$ are obtained by successive application of DP coding, where for each m, the interference I_m is noncausally known. This particular choice of precoding matrix $\mathbf{W} = \mathbf{Q}^*$ nulls interference caused by users $j > m$ and DP coding nulls interference caused by users $j < m$ so that the scheme forces all interference to zero. Hence, it was dubbed ZF-DP coding. The throughput of the ZF-DP scheme is given by [1]

$$R_{\mathrm{zfdp}} = \sum_{m=1}^{N} [\log_2(\mu d_m)]_+ \quad (10)$$

where $[x]_+ = \max\{0, x\}$, $d_n := |l_{n,n}|^2$, and μ is the solution of the water-filling equation

$$\sum_{m=1}^{N} \left[\mu - \frac{1}{d_m}\right]_+ = P. \quad (11)$$

Then, for $m = 1, \ldots, N$

$$p_m = d_m \left[\mu - \frac{1}{d_m}\right]_+. \quad (12)$$

Note that when $N < M$, one has to select up to N out of M users whose data will be transmitted. In general, different selections yield different values of R_{zfdp} in (10). Furthermore, different ordering within the same set of users yields different sum rate. The ZF-DP scheme does not attempt to optimize the throughput with respect to either user selection or ordering. In [13], Tu and Blum have proposed a greedy algorithm for the selection of N out of M rows of the channel matrix $\mathbf{H}$ and ordering of the selected rows in the Gram-Schmidt orthogonalization, aiming to maximize the throughput. The algorithm is called greedy ZF-DP and is presented here for convenience.

Let $U = \{1, 2, \ldots, M\}$ denote the set of indices of all M users, and let $S_n = \{s_1, \ldots, s_n\} \subset U$ denote the set of n selected users ($|S_n| = n$).

1) **Initialization:**
- Set $n = 1$.
- Let $r_{1,u} = \mathbf{h}_u \mathbf{h}_u^*$. Find a user s_1 such that $s_1 = \arg\max_{u \in U} r_{1,u}$.
- Set $S_1 = \{s_1\}$.

2) **While** $n < N$:
- Increase n by 1.
- Project each remaining channel vector onto the orthogonal complement of the subspace spanned by the channels of the selected users. The projector matrix is

$$\mathbf{P}_n^{\perp} = \mathbf{I}_N - \mathbf{H}(S_{n-1})^* \left(\mathbf{H}(S_{n-1})\mathbf{H}(S_{n-1})^*\right)^{-1} \mathbf{H}(S_{n-1}) \quad (13)$$

where $\mathbf{I}_N$ is the $N \times N$ identity matrix, and $\mathbf{H}(S_{n-1})$ denotes the row-reduced channel matrix consisting of the channel vectors of the users selected in the first $n-1$ steps

$$\mathbf{H}(S_{n-1}) = [\mathbf{h}_{s_1}^* \quad \mathbf{h}_{s_2}^* \quad \ldots \quad \mathbf{h}_{s_{n-1}}^*]^*. \quad (14)$$

Let $r_{n,u} = \left|\mathbf{h}_u \mathbf{P}_n^{\perp}\right|^2$. Due to idempotence of $\mathbf{P}_n^{\perp}$, we have

$$r_{n,u} = \mathbf{h}_u \mathbf{P}_n^{\perp} \mathbf{h}_u^*. \quad (15)$$

- Find a user s_n such that

$$s_n = \arg\max_{u \in U \setminus S_{n-1}} r_{n,u}. \quad (16)$$

- Set $S_n = S_{n-1} \cup \{s_n\}$.

3) **Beamforming:** Let $\mathbf{W} = \mathbf{Q}^*$, where $\mathbf{H}(S_N) = \mathbf{LQ}$ is the QR-type decomposition of $\mathbf{H}(S_N)$.

4) **DP coding**: Applied to the rows of $\mathbf{L}$.

Power Loading: Water-filling.

The rows $\mathbf{q}_m$ of $\mathbf{Q}$ in the QR decomposition of $\mathbf{H}(S_n) = \mathbf{L}(S_n)\mathbf{Q}(S_n)$ are obtained by applying Gram–Schmidt orthogonalization to the ordered rows of $\mathbf{H}(S_n)$: $\mathbf{h}_{s_1}, \ldots, \mathbf{h}_{s_n}$. This yields [1]

$$\mathbf{h}_{s_n} = \sqrt{\mathbf{h}_{s_n} \mathbf{P}_n^{\perp} \mathbf{h}_{s_n}^*}\, \mathbf{q}_{s_n} + \sum_{j \in S_{n-1}} \mathbf{h}_{s_n} \mathbf{q}_j^* \mathbf{q}_j. \quad (17)$$

From $\mathbf{L}(S_n) = \mathbf{H}(S_n)\mathbf{Q}(S_n)^*$, we obtain $l_{n,n} = \mathbf{h}_{s_n}\mathbf{q}_{s_n}^*$. By definition of d_n (10), orthonormality of $\mathbf{Q}(S_n)$, and (17), we have

$$d_n = |l_{n,n}|^2 = \mathbf{h}_{s_n}\mathbf{P}_n^{\perp}\mathbf{h}_{s_n}^*.$$

From (15) and (16), it follows that

$$d_n = \max_{u \in U \setminus S_{n-1}} r_{n,u} \tag{18}$$

for $n = 1, \ldots, N$. In other words, the gZF-DP algorithm maximizes d_n, conditioned on the choice of $d_1, \ldots, d_{n-1}$.

B. ZF With User Selection

ZF beamforming inverts the channel matrix at the transmitter so that orthogonal channels between transmitter and receivers are created. It is then possible to encode users individually, as opposed to the more complex long-block-vector coding generally needed to implement DP. Note that ZF at the transmitter does not enhance noise at the receiver, but it incurs an excess transmission power penalty relative to ZF-DP. If $M \leq N$, and $rank(\mathbf{H}) = M$, then the ZF beamforming matrix is

$$\mathbf{W} = \mathbf{H}^*(\mathbf{H}\mathbf{H}^*)^{-1} \tag{19}$$

which is the Moore-Penrose pseudoinverse of the channel matrix. However, if $M > N$, it is not possible to use (19) because $\mathbf{H}\mathbf{H}^*$ is singular. In that case, one needs to select $n \leq N$ out of M users.

For $M > N$, the problem (8) is reformulated as follows: Given $\mathbf{H} \in \mathbb{C}^{M \times N}$, select $n \leq N$ and a set of channels $\{\mathbf{h}_{s_1}, \ldots, \mathbf{h}_{s_n}\}$, which produce the row-reduced channel matrix

$$\mathbf{H}(S_n) = [\,\mathbf{h}_{s_1}^* \quad \mathbf{h}_{s_2}^* \quad \ldots \quad \mathbf{h}_{s_n}^*\,]^*$$

such that the sum rate is the highest achievable:

$$\max_{1 \leq n \leq N} \quad \max_{S_n} R_{zf}(S_n)$$
$$\text{subject to} \quad \sum_{i \in S_n} \left[\mu - \frac{1}{c_i(S_n)}\right]_+ = P. \tag{20}$$

The throughput of ZF algorithm is given by [1]

$$R_{zf}(S_n) = \sum_{i \in S_n} [\log_2(\mu c_i(S_n))]_+ \tag{21}$$

where

$$c_i(S_n) = \left\{ \left[(\mathbf{H}(S_n)\mathbf{H}(S_n)^*)^{-1} \right]_{i,i} \right\}^{-1} \tag{22}$$

and μ is obtained by solving the water-filling equation in (20). The power-loading then yields

$$p_i = c_i(S_n)\left[\mu - \frac{1}{c_i(S_n)}\right]_+, \quad \forall\, i \in S_n. \tag{23}$$

The problem can be conceptually solved by exhaustive search: For each value of n, find all possible n-tuples S_n and select a pair (n, S_n), which yields maximum $R_{zf}(S_n)$. However, such an algorithm has prohibitive complexity.

We propose a reduced-complexity suboptimal algorithm, dubbed ZF with Selection (ZFS), as outlined next.

1) **Initialization:**
- Set $n = 1$.
- Find a user, s_1, such that

$$s_1 = \arg\max_{u \in U} \mathbf{h}_u\mathbf{h}_u^*.$$

- Set $S_1 = \{s_1\}$ and denote the achieved rate $R_{zf}(S_1)_{\max}$.

2) **While** $n < N$:
- Increase n by 1.
- Find a user, s_n, such that

$$s_n = \arg\max_{u \in U \setminus S_{n-1}} R_{zf}(S_{n-1} \cup \{u\}).$$

- Set $S_n = S_{n-1} \cup \{s_n\}$, and denote the achieved rate $R_{zf}(S_n)_{\max}$.
- If $R_{zf}(S_n)_{\max} \leq R_{zf}(S_{n-1})_{\max}$ **break**, and decrease n by 1

3) **Beamforming:** $\mathbf{W} = \mathbf{H}(S_n)^*(\mathbf{H}(S_n)\mathbf{H}(S_n)^*)^{-1}$
Power Loading: Water-filling.

C. Complexity and Implementation

We consider complexity of the user selection procedure only. The complexity of DP coding, required by the gZF-DP algorithm, depends on its implementation, in particular, the degree of approximation and the associated spatio-temporal block length (which is a function of SNR), cf. [4], [18].

Complexity of the user selection procedure of the gZF-DP algorithm is $O(N^3M)$. To see this, note that for each $n \leq N$, the algorithm evaluates $M - n + 1$ 2-norms $r_{n,u}$. Evaluation of $r_{n,u}$ involves a vector-matrix multiplication, where the vector is $1 \times N$ and the matrix $N \times N$. The complexity of this step is $O(N^2)$. Repeating this over $O(M)$ users in N steps, we obtain $O(N^3M)$.

We will show that the complexity of the user selection procedure of the ZFS algorithm is also $O(N^3M)$. Again, for each $n \leq N$, the ZFS algorithm evaluates $M - n + 1$ rates $R_{zf}(S_{n-1} \cup \{u\})$. The evaluation of $R_{zf}(S_{n-1} \cup \{u\})$ is split into the evaluation of the $c_i(S_{n-1} \cup \{u\})$'s followed by evaluation of μ; cf. (21). An efficient way to evaluate the $c_i(S_{n-1} \cup \{u\})$'s is by using the matrix inversion lemma to invert the matrix $\mathbf{A}(S_{n-1} \cup \{u\}) := \mathbf{H}(S_{n-1} \cup \{u\})\mathbf{H}(S_{n-1} \cup \{u\})^*$. Note that

$$\mathbf{A}(S_{n-1} \cup \{u\}) = \begin{bmatrix} \mathbf{A}(S_{n-1}) & \mathbf{a}_u \\ \mathbf{a}_u^* & a_{u,u} \end{bmatrix}$$

where $\mathbf{a}_u = [\mathbf{h}_{s_1}\mathbf{h}_u^*,\ \mathbf{h}_{s_2}\mathbf{h}_u^*,\ \ldots\ \mathbf{h}_{s_{n-1}}\mathbf{h}_u^*]^T$, and $a_{u,u} = \mathbf{h}_u\mathbf{h}_u^*$. Noting that $\mathbf{A}(S_{n-1})^* = \mathbf{A}(S_{n-1})$ and writing

$$\mathbf{q} = \mathbf{A}(S_{n-1})^{-1}\mathbf{a}_u \tag{24}$$

after some algebraic manipulation, we obtain

$$\mathbf{A}(S_{n-1} \cup \{u\})^{-1} = \begin{bmatrix} \mathbf{A}(S_{n-1})^{-1} & \mathbf{0}_{n-1} \\ \mathbf{0}_{n-1}^T & 0 \end{bmatrix} + (a_{u,u} - \mathbf{a}_u^*\mathbf{q})^{-1} \begin{bmatrix} \mathbf{q}\mathbf{q}^* & -\mathbf{q} \\ -\mathbf{q}^* & 1 \end{bmatrix} \tag{25}$$

where $\mathbf{0}_{n-1}^T = [0 \quad 0 \quad \ldots \quad 0]_{1 \times (n-1)}$. It can be verified that each time n is increased, $\mathbf{A}(S_{n-1})^{-1}$ and $a_{i,u},\ i \in S_{n-2}$ are known before the search over $u \in U \setminus S_{n-1}$ starts. Hence, evaluation of $\mathbf{A}(S_{n-1} \cup \{u\})^{-1}$ from (24) and (25) has complexity proportional to $O(n^2)$. Repeating this over $O(M)$ users in each of $n \leq N$ steps, we obtain the overall complexity of the user-selection procedure of the ZFS algorithm to be $O(N^3 M)$.

It can be shown that the per-iteration complexity of the sum power iterative water-filling algorithm proposed by Jindal *et al.* [7] is $O(N^2 M^2)$. Therefore, the gZF-DP and ZFS algorithms have significantly lower computational complexity than the sum power iterative water-filling algorithm if $M \gg N$.

In the following, we pay attention to the substeps in step 2) of the ZFS algorithm. Given a set S_n, we have [1]

$$c_i(S_n) = |\mathbf{h}_{s_i} \mathbf{P}(S_n \setminus \{s_i\})^{\perp}|^2 \tag{26}$$

where $\mathbf{P}(S_n)^{\perp}$ denotes the projector onto the orthogonal complement of $\Omega(S_n) = \text{span}\{\mathbf{h}_{s_l} : s_l \in S_n\}$. Note that $c_j(S_{n-1} \cup \{u\}) \leq c_j(S_{n-1})$ for every user $j \in S_{n-1}$. This is due to (26) and $S_{n-1} \subset S_{n-1} \cup \{u\}$. Therefore, if (20) and (23) yield $p_u = 0$, then $R_{zf}(S_{n-1} \cup \{u\}) < R_{zf}(S_{n-1})$. We discard such u. We also discard u if (20) and (23) yield $p_{s_i} = 0$ for some $s_i \in S_{n-1}$. This is done to keep complexity at bay for otherwise, combinatorial search might effectively emerge. Hence, user u is a candidate for S_n if $p_i > 0, \forall\, i \in S_{n-1} \cup \{u\}$. From the properties of water-filling, this holds if

$$\frac{n}{c_{i_{\min}}(S_{n-1} \cup \{u\})} < P + \sum_{i \in S_{n-1} \cup \{u\}} \frac{1}{c_i(S_{n-1} \cup \{u\})} \tag{27}$$

where $c_{i_{\min}}(S_{n-1} \cup \{u\}) = \min_{i \in S_{n-1} \cup \{u\}} c_i(S_{n-1} \cup \{u\})$. Then, we have

$$\mu = \frac{1}{n}\left[P + \sum_{i \in S_{n-1} \cup \{u\}} \frac{1}{c_i(S_{n-1} \cup \{u\})}\right]. \tag{28}$$

If (27) is not satisfied, we skip to the next u.

We note that the **break** in Step 2 is necessary when ZFS is used but redundant when ZF-DP is used; it is shown in [1] and [13] that in the latter case, maximum sum rate can always be achieved with N active users if $P > 0$ [1]. On the other hand, when ZF alone is used, the optimum number of active users is $n_{opt} \leq N$ and decreases as P decreases, so that for $P \rightarrow 0$, the ZF scheme reduces to maximum ratio combining (MRC) $n_{opt} = 1$ [1]. This also holds for the proposed ZFS algorithm, which follows from the water-filling equation in (20) and the fact that $c_1(S_1) = \max_{i \in U} a_{i,i}$.

IV. Performance Analysis in Independent Rayleigh Fading

In this section, we evaluate the throughput of the greedy ZF-DP algorithm [13] in independent Rayleigh fading when channels remain constant over the duration of a transmission of a block of symbols. The channels of all M users are assumed to have i.i.d. entries, which are circularly symmetric, zero-mean, complex Gaussian random variables (r.v.s) with unit variance $h_{m,n} \sim \mathcal{CN}(0,1)$. In [1], the average throughput of the ZF-DP and ZF schemes in independent Rayleigh fading under a long-term power constraint for general N and M is evaluated. As noted earlier, the simple ZF-DP and ZF algorithms in [1] do not attempt to optimize throughput with respect to user selection and ordering when $M > N$. Instead, users are selected and ordered randomly.

A. gZF-DP Sum Rate Under Long-Term Power Constraint

We model the greedy ZF-DP algorithm [13] under a long-term power constraint. We are interested in evaluating

$$R_{gZF\text{-}DP} = E\left[\sum_{i=1}^{N} [\log(\mu_o d_i)]_+\right] \tag{29}$$

where μ_o is the solution of the water-filling equation, stemming from the long-term (LT) power constraint

$$E\left[\sum_{i=1}^{N}\left[\mu - \frac{1}{d_i}\right]_+\right] = P. \tag{30}$$

Note that the optimum μ_o determined by (30) will be a *deterministic function* of the statistics of the d_i's and not a function of the random variables themselves. By this and linearity of expectation, we can rewrite (29) as

$$\begin{aligned} R_{gZF\text{-}DP} &= \sum_{i=1}^{N} E[\log(\mu_o d_i)]_+ \\ &= \sum_{i=1}^{N} \int_0^{\infty} [\log(\mu_o x)]_+ f_{d_i}(x) dx. \end{aligned}$$

Therefore

$$R_{gZF\text{-}DP} = \sum_{i=1}^{N} \int_{1/\mu_o}^{\infty} \log(\mu_o x) f_{d_i}(x) dx \tag{31}$$

where $f_{d_i}(x)$ denotes the probability density function (pdf) of d_i. Similarly, (30) becomes

$$\sum_{i=1}^{N}\left(\mu \int_{1/\mu}^{\infty} f_{d_i}(x) dx - \int_{1/\mu}^{\infty} \frac{1}{x} f_{d_i}(x) dx\right) = P. \tag{32}$$

In order to evaluate R, we need to evaluate the pdfs of d_i's based on the knowledge of channel statistics and selection procedure. Our derivation below draws in part from performance analysis tools in [5], [17], which we tailor to fit the context of gZF-DP. In particular, our analysis accounts for and exploits the specific selection procedure employed in gZF-DP.

B. Probability Density Functions

It is instructive to consider the modeling of the pdf of d_1 first, followed by modeling the pdf of d_2, and then generalizing to compute the pdf of d_n for general $n \leq N$. First, let us determine the distribution of $r_{1,u} = \mathbf{h}_u \mathbf{h}_u^*$. Note that $r_{1,u}$ is a sum of N squared magnitudes of circularly symmetric, zero-mean, unit-variance complex Gaussian random variables. Therefore, it has Chi-squared distribution with $2N$ degrees of freedom ($r_{1,u} \sim \chi^2_{2N}$), whose pdf is

$$f_{r_1}(x_1) = \frac{1}{\Gamma(N)} x_1^{N-1} \exp(-x_1). \tag{33}$$

$\Gamma(N)$ denotes the Gamma function, and $\Gamma(N) = (N-1)!$ for a positive integer N. According to the selection algorithm

$$d_1 = \max_{u \in U} r_{1,u}. \quad (34)$$

From order statistics, e.g., [3, (2.1.1)], we obtain the pdf of d_1 as

$$f_{d_1}(x_1) = M\left[F_{r_1}(x_1)\right]^{M-1} f_{r_1}(x_1) \quad (35)$$

where $F_{r_1}(x_1)$ is the cumulative distribution function (cdf) of $r_{1,u}$. We say that the distribution of $r_{1,u}$ is the *parent distribution* of the order statistics $r_{1,(1)} \geq r_{1,(2)} \geq \cdots \geq r_{1,(M)}$, where $r_{1,(i)}$ is the ith largest $r_{1,u}$ for $u \in U$.

Noting that $r_{1,u} \leq d_1$, for all of the remaining users ($u \in U \setminus S_1$), it follows that the posterior distribution of $r_{1,u}$ of the remaining users (after selecting user s_1) depends on the realization of d_1. In the sequel, we will need to use the conditional pdf of $r_{1,u}$ of the remaining users given a realization of d_1. According to (34) and, e.g., [3, Th. 2.7], the parent distribution of the order statistics of the remaining users $u \in U \setminus S_1$ is equal to $f_{r_1}(x_1)$ truncated on the right at the value of d_1

$$f_{r_1|d_1}(x_1|y_1) = \begin{cases} \frac{f_{r_1}(x_1)}{F_{r_1}(y_1)}, & \text{if } x_1 \in [0, y_1] \\ 0, & \text{otherwise.} \end{cases} \quad (36)$$

After setting $n = 2$, the selection algorithm proceeds by projecting the channel vectors of all of the remaining users onto the orthogonal complement of the subspace spanned by the channel vector of user s_1. From (15), we have $r_{2,u} = \mathbf{h}_u \mathbf{P}_2^{\perp} \mathbf{h}_u^*$, for $u \in U \setminus S_1$, where $\mathbf{P}_2^{\perp}$ is given in (13). The distribution of $r_{2,u}$ given d_1, which is denoted $f_{r_2|d_1}(x_2|y_1)$, then becomes the parent distribution of the order statistics $r_{2,(i)}$, given d_1 for $i \geq 2$. Therefore, we need a mapping from $f_{r_1|d_1}(x_1|y_1)$ to $f_{r_2|d_1}(x_2|y_1)$ that models the projection step

$$f_{r_2|d_1}(x_2|y_1) = \int_0^{\infty} f_{r_2|r_1,d_1}(x_2|v, y_1) f_{r_1|d_1}(v|y_1)\,dv. \quad (37)$$

Here, $f_{r_2|r_1,d_1}(x_2|v, y_1)$ denotes the pdf of $r_{2,u}$, given realizations of $r_{1,u}$ and d_1. Note that $r_{2,u} \leq r_{1,u} \leq d_1$. $\mathbf{h}_{s_1}$ is statistically independent of $\mathbf{h}_u$, for $u \in U \setminus S_1$, so that from the point of view of the users in $U \setminus S_1$, $\mathbf{P}_2^{\perp}$ appears to be a randomly selected projector matrix. However, the first user has been selected after considering the channels of *all* users, and thus, there might be mild dependence between the channels of the remaining users in $U \setminus S_1$ and $\mathbf{P}_2^{\perp}$. For analytical tractability, we will ignore this dependence. Our simulation results will fully corroborate this approximation: The difference is not even noticeable in simulations.

Assumption 1: We therefore assume that d_1 conveys no information about $\mathbf{P}_2^{\perp}$, i.e., $f_{r_2|r_1,d_1}(x_2|v, y_1)$ has the Markovian property

$$f_{r_2|r_1,d_1}(x_2|v, y_1) = f_{r_2|r_1}(x_2|v). \quad (38)$$

The pdf $f_{r_2|r_1}(x_2|v)$ is obtained from the following.

Claim 1: Let $\mathbf{h} = [h_1 \ \ldots \ h_N]$ and $\mathbf{p} = [p_1 \ \ldots \ p_N]$ denote independent N-dimensional random (row-) vectors with i.i.d., circularly symmetric, zero-mean, complex Gaussian entries with unit variance $h_n \sim \mathcal{CN}(0,1)$ and $p_n \sim \mathcal{CN}(0,1)$. Let $Y := \mathbf{h}\mathbf{h}^*$ and $X := \mathbf{h}\mathbf{P}\mathbf{h}^*$, where $\mathbf{P} = \mathbf{I}_N - \mathbf{p}^*\left(\mathbf{p}\mathbf{p}^*\right)^{-1}\mathbf{p}$ [cf. (13)] is an $N \times N$ projector matrix with $N-1$ eigenvalues equal to 1 and one eigenvalue equal to 0. Then, the cdf of X, given Y, is given by

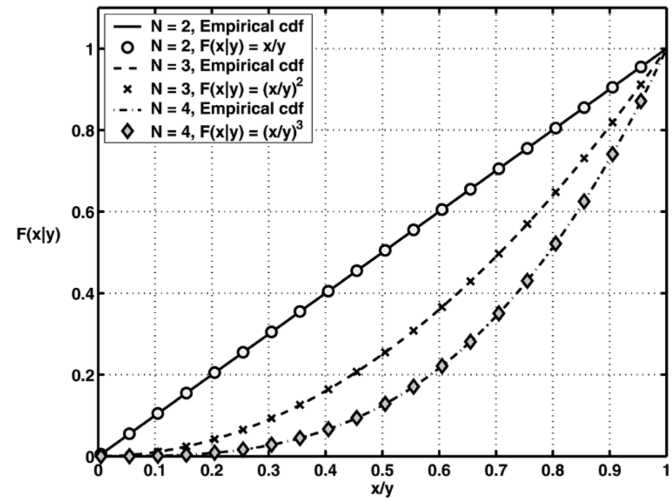

Fig. 1. cdf $F_{r_{n+1}|r_n}(x|y)$ when y : $1 \times N$ channel vector.

$$F_{X|Y}(x|y) = \begin{cases} \left(\frac{x}{y}\right)^{N-1}, & \text{for } x \in [0, y] \\ 0, & \text{elsewhere.} \end{cases} \quad (39)$$

Remark 1: The rigorous proof of this claim turned out to be elusive, but it is *very* well supported by simulations. Fig. 1 depicts $F_{X|Y}(x|y)$ versus x/y for $N = 2$, 3, and 4. Lines show empirical cdfs obtained by Monte Carlo (MC) simulations, and markers show samples of analytic curves given by (39). In MC simulations, for each value of N, there were 2×10^5 random realizations of $\mathbf{P}$ given $\mathbf{h}$, for 10^2 realizations of $\mathbf{h}$. The empirical $F_{X|Y}(x|y)$ is discrete. Its support $x/y \in [0, 1]$ is divided into 200 intervals of length 1/200. The match in Fig. 1 is very accurate.

From (39), we obtain

$$f_{r_2|r_1}(x_2|v) = \begin{cases} \frac{N-1}{v}\left(\frac{x_2}{v}\right)^{N-2}, & \text{for } x_2 \in [0, v], \\ 0, & \text{otherwise.} \end{cases} \quad (40)$$

From (18), it follows that d_2, conditioned on a realization of d_1, is the maximum of $M-1$ r.v.s with the parent distribution given by the pdf $f_{r_2|d_1}(x_2|x_1)$ from (37). Using order statistics, we obtain [3]

$$f_{d_2|d_1}(x_2|x_1) = (M-1)\left[F_{r_2|d_1}(x_2|x_1)\right]^{M-2} f_{r_2|d_1}(x_2|x_1). \quad (41)$$

Since $f_{r_2|d_1}(x_2|x_1) = 0$ for $x_2 > x_1$, it follows that $d_2 \leq d_1$. Finally

$$f_{d_2}(x_2) = \int_{x_1=0}^{\infty} f_{d_2|d_1}(x_2|x_1) f_{d_1}(x_1)\,dx_1 \quad (42)$$

for $x_1 \geq x_2$.

Armed with these insights, we can now generalize to the computation of the pdf of d_n for $n \leq N$. The associated derivation is deferred to the Appendix. Using the results of Section IV-A, the pdf of d_n is obtained as a marginal distribution:

$$f_{d_n}(x_n) = \int_{x_1=x_n}^{\infty} \int_{x_2=x_n}^{x_1} \cdots \int_{x_{n-1}=x_n}^{x_{n-2}} \cdot f_{d_n|d_{n-1},\ldots,d_1}(x_n|x_{n-1},\ldots,x_1) \cdot \prod_{k=2}^{n-1} f_{d_k|d_{k-1},\ldots,d_1}(x_k|x_{k-1},\ldots,x_1) \cdot f_{d_1}(x_1)dx_n \ldots dx_1 \quad (43)$$

for $x_1 \geq x_2 \geq \cdots x_n$.

The pdfs of d_n for $n = 1, \ldots, N$ can be written in a more compact form, facilitating analysis and numerical integration.

Proposition 1: Define

$$\phi_1(x_1) = f_{r_1}(x_1) \quad (44)$$

and

$$\phi_n(x_n, x_{n-1}, \ldots, x_1) = \frac{1}{\Gamma(N-n+1)} x_n^{N-n} \cdot \int_{v_{n-1}=x_n}^{x_{n-1}} \int_{v_{n-2}=v_{n-1}}^{x_{n-2}} \cdots \int_{v_1=v_2}^{x_1} \exp(-v_1) \cdot dv_1 \ldots dv_{n-1}. \quad (45)$$

Then, we have (46), shown at the bottom of the page. The proof is given in the Appendix. We will use the forms in the above proposition in the Proof of Theorem 1, whose statement appears in Section IV-C.

Fig. 2 depicts an example of pdfs of d_n for $N = 4$ and $M = 8$. Full lines depict analytically obtained pdfs. Markers show samples of the empirically obtained pdfs through Monte Carlo (MC) simulations. There are 10^6 MC samples. For every d_n, the support of the empirical pdf is truncated where the tail becomes insignificant. Then, the empirical pdf is discretized by dividing the truncated support into 100 equal intervals. These results justify the approximation (Assumption 1) made in the course of an analytical derivation for tractability considerations.

C. Throughput of gZF-DP at High SNR

Let $R_{gZF\text{-}DP}$ denote the average throughput of the gZF-DP algorithm. Let $\rho = 10\log_{10} P$ denote the SNR, where the noise variance of each user is assumed equal to 1. We have the following result.

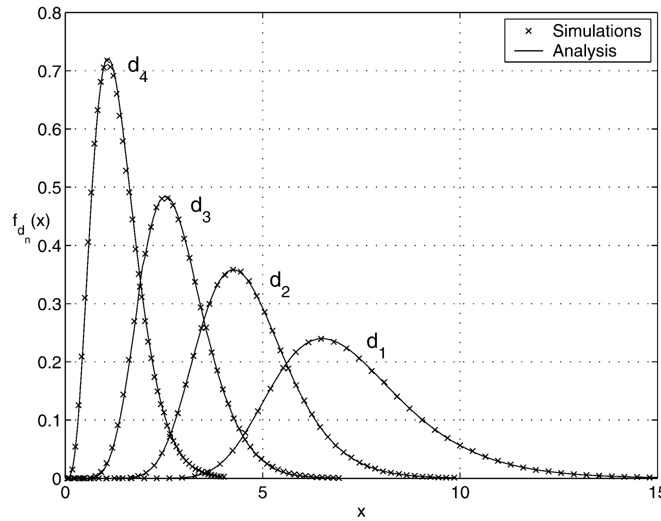

Fig. 2. Family of pdfs of d_n for $N = 4$, $M = 8$.

Theorem 1: Let $N < M$, and let P be the power limit. Then, under our working assumptions

$$\lim_{P\to\infty} \frac{\partial}{\partial\rho} R_{gZF\text{-}DP} = N\frac{\log_2 10}{10} \left[\frac{\text{bits}}{\text{dB}}\right]. \quad (47)$$

The proof is given in the Appendix. The above theorem shows that the throughput versus SNR slope of the gZF-DP algorithm in the high SNR regime is proportional to the number of antennas at the transmitter N. Note that this is the theoretical limit of the capacity versus SNR slope for a multiple-input multiple-output (MIMO) system with N transmit and $M > N$ receive antennas [9].

V. Comparison of Greedy ZF-DP and ZFS

The throughputs of the gZF-DP and ZFS algorithms are presented in Figs. 3 and 4. The y-axis shows sum capacity and sum rate in bits per channel use. The x-axis shows total power P in decibels. The noise level of every user is 1. The sum capacity and sum rates are averaged over 100 channels. Channels are complex-valued, drawn from an i.i.d. Rayleigh distribution with unit-variance for each channel entry. The sum capacity is obtained using the approach proposed in [14].

For the gZF-DP algorithm, analysis (obtained under a long-term power constraint) yields throughput very close to that obtained via simulations (under a short-term power constraint). This can be explained as follows. Capitalizing on multiuser diversity, gZF-DP selects and orders channels (users) from a large pool of statistically independent candidates. The result is that the ensuing d_i's are far more stable than they would have been

$$f_{d_n}(x_n) = \frac{M!}{(M-n)!} \int_{x_1=x_n}^{\infty} \int_{x_2=x_n}^{x_1} \cdots \int_{x_{n-1}=x_n}^{x_{n-2}} \left[\int_{y=0}^{x_n} \phi_n(y, x_{n-1}, \ldots, x_1)dy\right]^{M-n} \cdot \prod_{k=1}^{n} \phi_k(x_k, \ldots, x_1)dx_{n-1} \ldots dx_1. \quad (46)$$

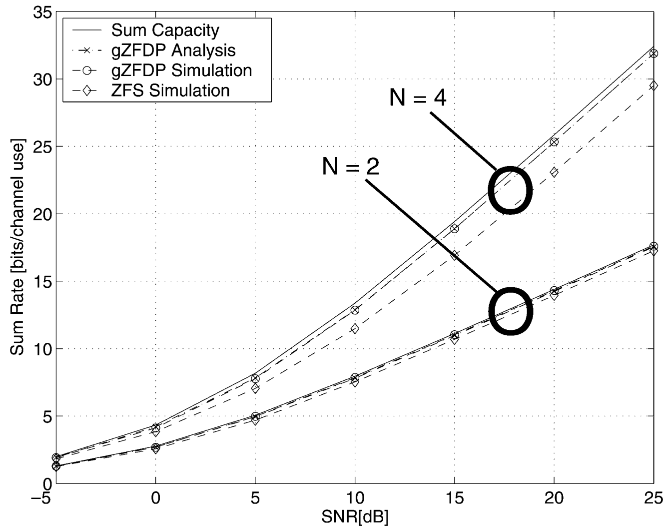

Fig. 3. ZFS versus Greedy ZF-DP versus Sum capacity: $M = 8$ users, $N = 2$, and $N = 4$.

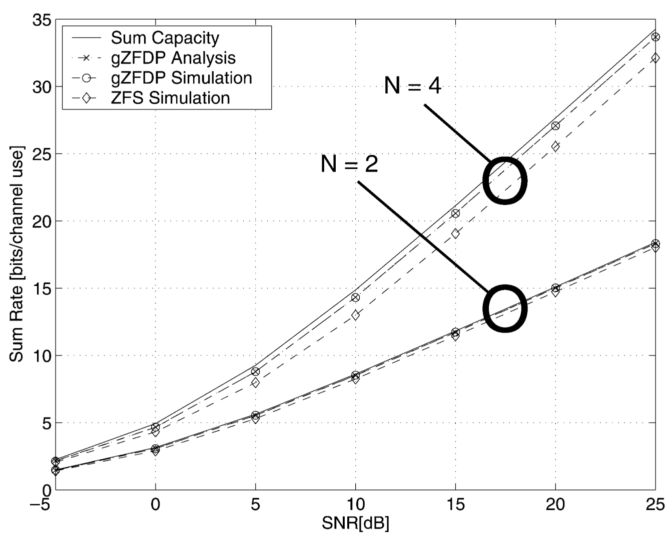

Fig. 4. ZFS versus Greedy ZF-DP versus Sum Capacity: $M = 16$ users, $N = 2$, and $N = 4$.

without user selection and ordering. This justifies the use of a long-term power constraint for analysis, as opposed to the short-term power constraint originally proposed in the algorithm and used in simulations.

In these scenarios ($N = 2$ or 4 and $M = 8$ or 16), both gZF-DP and ZFS algorithms achieve throughput close to sum capacity. Note that ZFS exhibits the same slope of rate increase per decibel of SNR as the gZF-DP algorithm and the sum capacity curve at moderate and high SNR.

Fig. 5 shows the throughput of the ZFS algorithm as a fraction of the throughput of the gZF-DP algorithm for various pairs N, M at 20 dB SNR. The curves are obtained by simulations, averaging over 2×10^4 channels for each pair N, M. For all N, M considered, this fraction stays between 0.875 and 0.985. For a given M, the gap between gZF-DP and ZFS increases as N increases, but even for $N = 8$, the gap is uniformly less than 13% of the gZF-DP throughput. Note that a realistic implementation of DP coding will incur a certain rate loss for the gZF-DP algorithm, so that the gap would be smaller in reality.

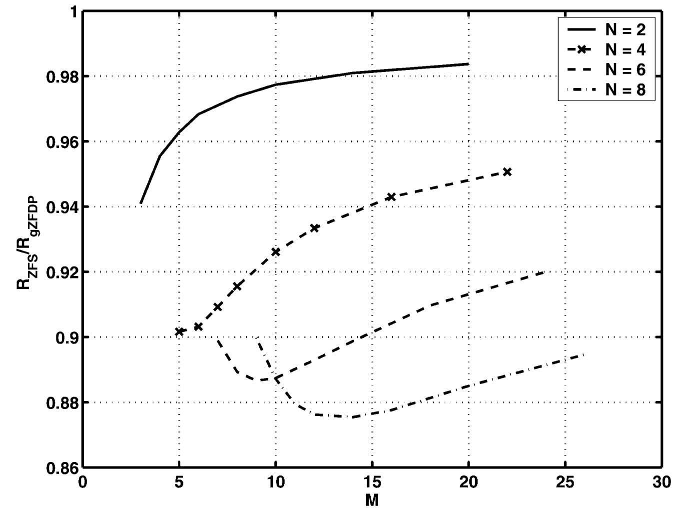

Fig. 5. $R_{ZFS}/R_{gZF\text{-}DP}$ for various numbers of antennas, N, and users, M, at 20 dB SNR.

Given N and for sufficiently large M, Fig. 5 shows that the gap between ZFS and gZF-DP decreases with M. This is due to multiuser diversity—the more users that contend for transmission, the higher the probability that N of them will be almost orthogonal. This in turn reduces the advantage of DP-coding-based schemes over ZFS. Depending on N, the fraction of sum rate of ZFS over the sum rate of gZF-DP may first exhibit a dip before starting to increase steadily with M. While the dip is small (less than 3%), it is noticeable, and we do not have an explanation for it. We have observed that, as SNR increases, more transmit antennas are required for this dip to occur.

VI. Conclusions

We have considered two algorithms that capitalize on multiuser diversity to achieve a significant fraction of the multiantenna downlink sum capacity when the number of users M is greater than the number of antennas N. We have analyzed the throughput performance of the greedy ZF-DP algorithm in independent Rayleigh fading and characterized the pdfs of certain key parameters of interest. Determining the proper number of samples required for accurate Monte Carlo estimates is a difficult issue without a baseline. While the end result of gZF-DP performance analysis requires sequential numerical integration and is admittedly cumbersome, it provides such a baseline and thus corroborates the results of Monte Carlo estimation. In addition, numerical integration is simpler than Monte Carlo simulation for a small number of transmit antennas. Furthermore, our analysis allowed us to establish that at high SNR, the throughput versus SNR slope of the gZF-DP algorithm is proportional to N.

We have also proposed another low-complexity algorithm, dubbed ZFS, which does not require DP coding at the transmitter. We have shown that the selection procedures of gZF-DP and ZFS algorithms have the same complexity order $O(N^3M)$, which is significantly smaller than the complexity of the optimal algorithms when $M \gg N$. We have evaluated the throughput performance of the ZFS algorithm via simulations. The results show that for a realistic number of transmit antennas, ZFS achieves a significant fraction of the throughput of gZF-DP and sum capacity at a low coding and online computation cost. The simulation results also indicate that at high SNR, ZFS achieves the same slope of throughput per decibel of SNR as the capacity-achieving strategy based on the use of DP coding for known interference cancellation and convex optimization.

Due to its simplicity, low complexity, and close to optimal performance, the proposed ZFS method offers an attractive alternative to earlier DP-based methods when $M \gg N$.

APPENDIX A
DERIVATION OF THE PDF OF d_n

Note that there are three basic steps in deriving $f_{d_n}(x_n)$:

1) *Truncation of the parent pdf after selecting user s_{n-1}*: Find the conditional pdf of $r_{n-1,u}$ of the remaining users ($u \in U \setminus S_{n-1}$) given realizations of $d_{n-1} \leq \cdots \leq d_1$. From order statistics [3], we obtain (48), shown at the bottom of the page.

2) *Mapping of $f_{r_{n-1}|d_{n-1},\ldots,d_1}(x_{n-1}|y_{n-1},\ldots,y_1)$ into $f_{r_n|d_{n-1},\ldots,d_1}(x_n|y_{n-1},\ldots,y_1)$*: Given realizations of d_i for $i = 1,\ldots,n-1$, where $n \leq N$, there are $n-1$ quadratic-form equations

$$d_i = \mathbf{h}_{s_i}\mathbf{P}_i^{\perp}\mathbf{h}_{s_i}^{*}.$$

Let the eigenvalue decomposition of $\mathbf{P}_i^{\perp}$ be

$$\mathbf{P}_i^{\perp} = \mathbf{U}_i\boldsymbol{\Theta}_i\mathbf{U}_i^{*}.$$

From (13), it follows that there are $N-i+1$ eigenvalues equal to 1 and $i-1$ eigenvalues equal to zero. Then, we can write

$$d_i = \sum_{j=1}^{N-i+1} |(\mathbf{h}_{s_i}\mathbf{U}_i)_j|^2.$$

As per Assumption 1, we neglect the (mild) dependence of the projector matrices $\mathbf{P}_i^{\perp}$ on the d_i's for $i = 1,\ldots,n-1$. This yields

$$f_{r_n|r_{n-1},d_{n-1},\ldots,d_1}(x_n|v,y_{n-1},\ldots,y_1) = f_{r_n|r_{n-1}}(x_n|v). \tag{49}$$

Since the projection $\mathbf{h}_u\mathbf{P}_n^{\perp}$ is a vector in an $N-n+1$-dimensional subspace, it follows from Claim 1 that

$$f_{r_n|r_{n-1}}(x_n|v) = \begin{cases} \frac{N-n+1}{v}\left(\frac{x_n}{v}\right)^{N-n}, & \text{for } x_n \in [0,v] \\ 0, & \text{otherwise.} \end{cases} \tag{50}$$

Then, the pdf of the parent distribution of $r_{n,u}$ of the remaining users given $d_{n-1} \leq \cdots \leq d_1$ is

$$f_{r_n|d_{n-1},\ldots,d_1}(x_n|y_{n-1},\ldots,y_1) = \int_0^{\infty} f_{r_n|r_{n-1}}(x_n|v) \cdot f_{r_{n-1}|d_{n-1},\ldots,d_1}(v|y_{n-1},\ldots,y_1)dv \tag{51}$$

where $x_n \leq v \leq y_{n-1} \leq \cdots \leq y_1$.

3) d_n conditioned on $d_{n-1},\ldots,d_1$ is the maximum of $M-n+1$ r.v.s with pdf given in (51). Using order statistics [3], we obtain

$$\begin{aligned} f_{d_n|d_{n-1},\ldots,d_1}&(x_n|x_{n-1},\ldots,x_1) \\ &= (M-n+1) \\ &\quad\cdot \left[F_{r_n|d_{n-1},\ldots,d_1}(x_n|x_{n-1},\ldots,x_1)\right]^{M-n} \\ &\quad\cdot f_{r_n|d_{n-1},\ldots,d_1}(x_n|x_{n-1},\ldots,x_1). \end{aligned} \tag{52}$$

APPENDIX B
PROOFS

Proof of Proposition 1: Let us first prove the following:

$$f_{r_n|d_{n-1},\ldots,d_1}(x_n|x_{n-1},\ldots,x_1) = \frac{\phi_n(x_n,x_{n-1},\ldots,x_1)}{\prod_{j=1}^{n-1} F_{r_j|d_{j-1},\ldots,d_1}(x_j|x_{j-1},\ldots,x_1)} \tag{53}$$

where $\phi_n(x_n,x_{n-1},\ldots,x_1)$ is given in (45).

This is proven by induction. For $n=2$, we have

$$f_{r_2|d_1}(x_2|x_1) = \int_{y=x_2}^{x_1} f_{r_2|r_1}(x_2|y)f_{r_1|d_1}(y|x_1)dy.$$

From (33), (36), and (40), we obtain

$$f_{r_2|d_1}(x_2|x_1) = \frac{1}{F_{r_1}(x_1)}\frac{1}{\Gamma(N-1)}x_2^{N-2}\int_{v_1=x_2}^{x_1}\exp(-v_1)\,dv_1.$$

From (45), it follows that

$$f_{r_2|d_1}(x_2|x_1) = \frac{\phi_2(x_2,x_1)}{F_{r_1}(x_1)}.$$

Induction hypothesis: (53).

Induction Step:

$$f_{r_{n+1}|d_n,\ldots,d_1}(x_{n+1}|x_n,\ldots,x_1) = \int_{v_n=x_{n+1}}^{x_n} f_{r_{n+1}|r_n}(x_{n+1}|v_n)f_{r_n|d_n,\ldots,d_1}(v_n|x_n,\ldots x_1)dv_n.$$

$$f_{r_{n-1}|d_{n-1},\ldots,d_1}(x_{n-1}|y_{n-1},\ldots,y_1) = \begin{cases} \frac{f_{r_{n-1}|d_{n-2},\ldots,d_1}(x_{n-1}|y_{n-2},\ldots,y_1)}{F_{r_{n-1}|d_{n-2},\ldots,d_1}(y_{n-1}|y_{n-2},\ldots,y_1)}, & x_{n-1} \leq y_{n-1} \leq \cdots \leq y_1 \\ 0, & \text{otherwise.} \end{cases} \tag{48}$$

From (48) and (50), we obtain

$$\begin{aligned} & f_{r_{n+1}|d_n,\ldots,d_1}(x_{n+1}|x_n,\ldots,x_1) \\ &\quad = F_{r_n|d_{n-1},\ldots,d_1}(x_n|x_{n-1},\ldots,x_1)^{-1} \\ &\quad \cdot \int_{v_n=x_{n+1}}^{x_n} \frac{N-n}{v_n}\left(\frac{x_{n+1}}{v_n}\right)^{N-n-1} \\ &\quad \cdot f_{r_n|d_{n-1},\ldots,d_1}(v_n|x_{n-1},\ldots,x_1)dv_n. \end{aligned}$$

By the induction hypothesis, we have

$$\begin{aligned} & f_{r_{n+1}|d_n,\ldots,d_1}(x_{n+1}|x_n,\ldots,x_1) \\ &\quad = \left[F_{r_n|d_{n-1},\ldots,d_1}(x_n|x_{n-1},\ldots,x_1)\right]^{-1} \\ &\quad \cdot \left[\prod_{j=1}^{n-1} F_{r_j|d_{j-1},\ldots,d_1}(x_j|x_{j-1},\ldots,x_1)\right]^{-1} \\ &\quad \cdot \int_{v_n=x_{n+1}}^{x_n} \frac{N-n}{v_n}\left(\frac{x_{n+1}}{v_n}\right)^{N-n-1} \\ &\quad \cdot \phi_n(v_n,x_{n-1},\ldots x_1)dv_n. \end{aligned}$$

From (45), it follows that

$$\begin{aligned} & f_{r_{n+1}|d_n,\ldots,d_1}(x_{n+1}|x_n,\ldots,x_1) \\ &\quad = \left[\prod_{j=1}^{n} F_{r_j|d_{j-1},\ldots,d_1}(x_j|x_{j-1},\ldots,x_1)\right]^{-1} \\ &\quad \cdot \frac{N-n}{\Gamma(N-n+1)} x_{n+1}^{N-n-1} \\ &\quad \cdot \int_{v_n=x_{n+1}}^{x_n} \int_{v_{n-1}=v_n}^{x_{n-1}} \cdots \int_{v_1=v_2}^{x_1} \exp(-v_1) \\ &\quad \cdot dv_1 \ldots dv_{n-1}dv_n. \end{aligned}$$

Applying (45) again, we have

$$f_{r_{n+1}|d_n,\ldots,d_1}(x_{n+1}|x_n,\ldots,x_1) = \frac{\phi_{n+1}(x_{n+1},x_n,\ldots,x_1)}{\prod_{j=1}^{n} F_{r_j|d_{j-1},\ldots,d_1}(x_j|x_{j-1},\ldots,x_1)}.$$

Now, we use the above result to prove Proposition 1. For $n = 1$, from (44), we obtain

$$f_{d_1}(x_1) = M\left[\int_{y=0}^{x_1}\phi_1(y)dy\right]^{M-1}\phi_1(x_1).$$

For $1 < n \le N$ and substituting (52) into (43), we obtain the equation shown at the bottom of the page. Applying (53), we obtain the equation at the top of the next page. Dividing the left fraction and rearranging the right one, we obtain

$$\begin{aligned} & G_{n-1}(x_{n-1},\ldots,x_1) \\ &\quad = \frac{\prod_{k=2}^{n-1}\left[F_{r_k|d_{k-1},\ldots,d_1}(x_k|x_{k-1},\ldots,x_1)\right]^{n-1-k}}{\prod_{j=1}^{n-2}\left[F_{r_j|d_{j-1},\ldots,d_1}(x_j|x_{j-1},\ldots,x_1)\right]^{n-1-j}} \\ &\quad \cdot \frac{1}{\left[F_{r_1}(x_1)\right]^{M-n+1}} \\ & G_{n-1}(x_{n-1},\ldots,x_1) \\ &\quad = \frac{1}{\left[F_{r_1}(x_1)\right]^{M-1}}. \end{aligned}$$

Therefore

$$\begin{aligned} & f_{d_n}(x) \\ &= \frac{M!}{(M-n)!} \\ &\quad \cdot \int_{x_1=x}^{\infty}\int_{x_2=x}^{x_1}\int_{x_{n-1}=x}^{x_{n-2}}\left[\int_{y=0}^{x_n}\phi_n(y,x_{n-1},\ldots,x_1)dy\right]^{M-n} \\ &\quad \cdot \prod_{k=1}^{n}\phi_k(x_k,\ldots,x_1)dx_{n-1}\ldots dx_1. \end{aligned}$$

■

Proof of Theorem:

$$\frac{\partial}{\partial\rho}R_{gZF\text{-}DP} = \sum_{i=1}^{N}\frac{\partial}{\partial\rho}R_i, \quad \text{where } \frac{\partial}{\partial\rho}R_i = \frac{\partial\mu}{\partial\rho}\frac{\partial}{\partial\mu}R_i.$$

$\rho = 10\log_{10}(P)$ so that from (32), we have

$$\begin{aligned} \frac{\partial\mu}{\partial\rho} &= \frac{\partial\mu}{\partial P}\frac{\partial P}{\partial\rho} \\ &= \frac{1}{N-\sum_{i=1}^{N}F_{d_i}\left(\frac{1}{\mu}\right)}\frac{\ln 10}{10}P. \end{aligned}$$

Using the Leibnitz rule, from (31), we have

$$\frac{\partial}{\partial\mu}R_i = \frac{1}{\mu\ln 2}\left(1-F_{d_i}\left(\frac{1}{\mu}\right)\right).$$

It follows that

$$\frac{\partial}{\partial\rho}R_{gZF\text{-}DP} = \frac{\log_2 10}{10}\frac{P}{\mu}.$$

In order to determine $\lim_{\rho\to\infty}(\partial/\partial\rho)R_{gZF\text{-}DP}$, we will determine $\lim_{\rho\to\infty}(P/\mu)$. Note that $\rho\to\infty$ is equivalent to $P\to\infty$. In addition, $(\partial P/\partial\mu) = N-\sum_{i=1}^{N}F_{d_i}(1/\mu) > 0$ for

---

$$\begin{aligned} f_{d_n}(x_n) = \frac{M!}{(M-n)!}\int_{x_1=x_n}^{\infty}\int_{x_2=x_n}^{x_1}\cdots\int_{x_{n-1}=x_n}^{x_{n-2}}&\left[F_{r_n|d_{n-1},\ldots,d_1}(x_n|x_{n-1},\ldots,x_1)\right]^{M-n} \\ \cdot f_{r_n|d_{n-1},\ldots,d_1}(x_n|x_{n-1},\ldots,x_1)&\prod_{k=2}^{n-1}\left[F_{r_k|d_{k-1},\ldots,d_1}(x_k|x_{k-1},\ldots,x_1)\right]^{M-k} \\ \cdot f_{r_k|d_{k-1},\ldots,d_1}(x_k|x_{k-1},\ldots,x_1)&\left[F_{r_1}(x_1)\right]^{M-1}f_{r_1}(x_1)dx_{n-1}\ldots dx_1. \end{aligned}$$

$$f_{d_n}(x_n) = \frac{M!}{(M-n)!}\int_{x_1=x_n}^{\infty}\int_{x_2=x_n}^{x_1}\cdots\int_{x_{n-1}=x_n}^{x_{n-2}}\left[\frac{\int_{y=0}^{x_n}\phi_n(y,x_{n-1},\ldots,x_1)dy}{\prod_{j=1}^{n-1}F_{r_j|d_{j-1},\ldots,d_1}(x_j|x_{j-1},\ldots,x_1)}\right]^{M-n}$$
$$\cdot\frac{\phi_n(x_n,\ldots,x_1)}{\prod_{j=1}^{n-1}F_{r_j|d_{j-1},\ldots,d_1}(x_j|x_{j-1},\ldots,x_1)}$$
$$\cdot\prod_{k=2}^{n-1}\left\{\left[F_{r_k|d_{k-1},\ldots,d_1}(x_k|x_{k-1},\ldots,x_1)\right]^{M-k}\frac{\phi_k(x_k,\ldots,x_1)}{\prod_{j=1}^{k-1}F_{r_j|d_{j-1},\ldots,d_1}(x_j|x_{j-1},\ldots,x_1)}\right\}$$
$$\cdot\left[F_{r_1}(x_1)\right]^{M-1}\phi_1(x_1)dx_{n-1}\ldots dx_1$$
$$f_{d_n}(x_n) = \frac{M!}{(M-n)!}$$
$$\cdot\int_{x_1=x_n}^{\infty}\int_{x_2=x_n}^{x_1}\cdots\int_{x_{n-1}=x_n}^{x_{n-2}}\left[\int_{y=0}^{x_n}\phi_n(y,x_{n-1},\ldots,x_1)dy\right]^{M-n}$$
$$\cdot\prod_{k=1}^{n}\phi_k(x_k,\ldots,x_1)G_{n-1}(x_{n-1},\ldots,x_1)\left[F_{r_1}(x_1)\right]^{M-1}dx_{n-1}\ldots dx_1$$

where

$$G_{n-1}(x_{n-1},\ldots,x_1) = \frac{\prod_{k=2}^{n-1}\left[F_{r_k|d_{k-1},\ldots,d_1}(x_k|x_{k-1},\ldots,x_1)\right]^{M-k}}{\prod_{j=1}^{n-1}\left[F_{r_j|d_{j-1},\ldots,d_1}(x_j|x_{j-1},\ldots,x_1)\right]^{M-n+1}}\frac{1}{\prod_{k=2}^{n-1}\prod_{j=1}^{k-1}F_{r_j|d_{j-1},\ldots,d_1}(x_j|x_{j-1},\ldots,x_1)}.$$

$\mu > 0$ so that $P \to \infty$ is equivalent to $\mu \to \infty$. We will prove that $\lim_{\mu\to\infty}(P/\mu) = N$. From (32), we have

$$\frac{P}{\mu} = \sum_{i=1}^{N}\int_{1/\mu}^{\infty}f_{d_i}(z)dz - \frac{1}{\mu}\sum_{i=1}^{N}\int_{1/\mu}^{\infty}\frac{1}{z}f_{d_i}(z)dz.$$

Then

$$\lim_{\mu\to\infty}\frac{P}{\mu} = N - \lim_{\mu\to\infty}\frac{1}{\mu}g_N(\mu)$$

where

$$g_N(\mu) = \sum_{i=1}^{N}\int_{1/\mu}^{\infty}\frac{1}{z}f_{d_i}(z)dz.$$

Note that if we demonstrate that

$$\lim_{\mu\to\infty}\frac{\partial}{\partial\mu}g_N(\mu) = 0$$

the desired result will follow because

$$\lim_{\mu\to\infty}\frac{\partial}{\partial\mu}g_N(\mu) = 0 \Rightarrow \lim_{\mu\to\infty}g_N(\mu) = O(1)$$
$$\Rightarrow \lim_{\mu\to\infty}\frac{1}{\mu}g_N(\mu) = 0$$
$$\Rightarrow \lim_{\mu\to\infty}\frac{P}{\mu} = N.$$

It is easy to check that $(\partial/\partial\mu)g_N(\mu) = \sum_{i=1}^{N}(1/\mu)f_{d_i}(1/\mu)$ so that it suffices to prove that $\lim_{\mu\to\infty}f_{d_i}(1/\mu) = 0$ or, equivalently, $\lim_{x\to 0}f_{d_i}(x) = 0$, for $i = 1,2,\ldots,N$, where $N \geq 2$, and $N < M$.

From (33) and (44), it follows that $\phi_1(0) = 0$. Then, from (35), it follows that $f_{d_1}(0) = 0$.

In order to prove that $f_{d_n}(0) = 0$ for $1 < n \leq N$, we will prove that $\phi_n(0,x_{n-1},\ldots,x_1)$ is bounded for any $0 \leq x_{n-1} \leq \cdots \leq x_1$. In order to prove that $\phi_n(0,x_{n-1},\ldots,x_1)$ is bounded, consider the multiple integral [cf. (45)]

$$I_n = \int_{v_{n-1}=0}^{x_{n-1}}\int_{v_{n-2}=v_{n-1}}^{x_{n-2}}\cdots\int_{v_1=v_2}^{x_1}\exp(-v_1)dv_1\ldots dv_{n-1}.$$

Integrating over dv_1, we obtain

$$I_n = \int_{v_{n-1}=0}^{x_{n-1}}\int_{v_{n-2}=v_{n-1}}^{x_{n-2}}\cdots\int_{v_2=v_3}^{x_2}\exp(-v_2)dv_2\ldots dv_{n-1}$$
$$-\exp(-x_1)\int_{v_{n-1}=0}^{x_{n-1}}\int_{v_{n-2}=v_{n-1}}^{x_{n-2}}\cdots\int_{v_2=v_3}^{x_2}dv_2\ldots dv_{n-1}$$
$$I_n = I_{n,1} - \exp(-x_1)B_{n,2}(x_{n-1},\ldots,x_2).$$

Observe that the first multiple integral on the right-hand side (RHS), which is denoted $I_{n,1}$, has the same form as I_n. Due to $x_1 \geq x_2 \geq \cdots \geq x_{n-1} \geq 0$, we have

$$B_{n,1}(x_{n-1},\ldots,x_2) \leq \int_{v_{n-1}=0}^{x_1}\int_{v_{n-2}=0}^{x_1}\cdots\int_{v_2=0}^{x_1}dv_2\ldots dv_{n-1}.$$

Therefore

$$B_{n,1}(x_{n-1},\ldots,x_2) \leq x_1^{n-2}.$$

Note that $\exp(-x_1)x_1^{n-2}$ is bounded for all $x_1 \geq 0$ so that $\exp(-x_1)B_{n,1}(x_{n-1},\ldots,x_2)$ is also bounded. Integrating over all dummy variables, we obtain

$$I_n = \exp(-x_{n-1}) - 1 - \sum_{j=1}^{n-2}\exp(-x_j)B_{n,j}(x_{n-j},\ldots,x_2)$$

where

$$B_{n,j}(x_{n-j},\ldots,x_{j+1}) = \int_{v_{n-1}=0}^{x_{n-1}}\cdots\int_{v_{j+1}=v_{j+2}}^{x_{j+1}} dv_{j+1}\ldots dv_{n-1}.$$

It can be shown that $\exp(-x_j)\, B_{n,j}(x_{n-1},\ldots,x_2)$ is bounded by the same argument as for $\exp(-x_1)\, B_{n,1}(x_{n-1},\ldots,x_2)$. Therefore, $\phi_n(0,x_{n-1},\ldots,x_1)$ is bounded for all $x_1 \geq x_2 \geq \cdots \geq x_{n-1} \geq 0$.

Then, from (45), it follows that

$$\phi_n(0,x_{n-1},\ldots,x_1) = \begin{cases} \frac{\int_{v_{n-1}=0}^{x_{n-1}}\cdots\int_{v_1=v_2}^{x_1}\exp(-v_1)dv_1\ldots dv_{n-1}}{\Gamma(N-n+1)}, & n=N \\ 0, & n<N. \end{cases}$$

If $n<N$, then from (43), it follows that $f_{d_n}(0)=0$. If $n=N$, then applying the mean-value theorem, we obtain

$$\lim_{x_n\to 0}\int_{y=0}^{x_n}\phi_n(y,x_{n-1},\ldots,x_1)dy = \lim_{x_n\to 0}\phi_n(0,x_{n-1},\ldots,x_1)x_n.$$

Since $\phi_n(0,x_{n-1},\ldots,x_1)$ is bounded

$$\lim_{x_n\to 0}\int_{y=0}^{x_n}\phi_n(y,x_{n-1},\ldots,x_1)dy = 0.$$

Finally, from (43) and $n=N<M$, it follows that $f_{d_N}(0)=0$. ■

REFERENCES

[1] G. Caire and S. Shamai (Shitz), "On the achievable throughput of a multi-antenna Gaussian broadcast channel," *IEEE Trans. Inf. Theory*, vol. 49, no. 7, pp. 1691–1706, Jul. 2003.

[2] M. H. M. Costa, "Writing on dirty paper," *IEEE Trans. Inf. Theory*, vol. IT-29, no. 3, pp. 439–441, May 1983.

[3] H. A. David, *Order Statistics*, 2nd ed. New York: Wiley, 1981.

[4] G. D. Forney Jr, "Trellis shaping," *IEEE Trans. Inf. Theory*, vol. 38, no. 2, pp. 281–300, Mar. 1992.

[5] D. Gore, R. W. Heath Jr, and A. Paulraj, "Transmit selection in spatial multiplexing systems," *IEEE Commun. Lett.*, vol. 6, no. 11, pp. 491–493, Nov. 2002.

[6] R. A. Horn and C. R. Johnson, *Matrix Analysis*. New York: Cambridge Univ. Press, 1985.

[7] N. Jindal, W. Rhee, S. Vishwanath, S. Jafar, and A. Goldsmith, "Sum power iterative waterfilling for Gaussian vector broadcast channels," *IEEE Trans. Inf. Theory*, submitted for publication.

[8] C. B. Peel, "On dirty paper coding," *Signal Process. Mag.*, vol. 20, no. 3, pp. 112–113, May 2003.

[9] W. Rhee and J. M. Cioffi, "On the capacity of multiuser wireless channels with multiple antennas," *IEEE Trans. Inf. Theory.*, vol. 49, no. 10, pp. 2580–2595, Oct. 2003.

[10] D. Samardzija and N. Mandayam, "Multiple antenna transmitter optimization schemes for multiuser systems," in *Proc. IEEE Veh. Technol. Conf.*, Orlando, FL, 2003, pp. 399–403.

[11] Q. Spencer and M. Haardt, "Capacity and downlink transmission algorithms for a multi-user MIMO channel," in *Proc. 36th Asilomar Conf. Signals, Syst., Comput.*, Pacific Grove, CA, Nov. 2002.

[12] I. E. Telatar, "Capacity of multi-antenna Gaussian channels," *Eur. Trans. Telecomm.*, vol. 10, no. 6, pp. 585–596, Nov.–Dec. 1999.

[13] Z. Tu and R. S. Blum, "Multiuser diversity for a dirty paper approach," *IEEE Commun. Lett.*, vol. 7, no. 8, pp. 370–372, Aug. 2003.

[14] S. Vishwanath, N. Jindal, and A. Goldsmith, "Duality, achievable rates and sum-rate capacity of Gaussian MIMO broadcast channels," *IEEE Trans. Inf. Theory*, vol. 49, no. 10, pp. 2658–2668, Oct. 2003.

[15] P. Viswanath and D. Tse, "Sum capacity of the vector Gaussian broadcast channel and uplink-downlink duality," *IEEE Trans. Inf. Theory*, vol. 49, no. 8, pp. 1912–1921, Aug. 2003.

[16] H. Viswanathan, S. Venkatesan, and H. Huang, "Downlink capacity evaluation of cellular networks with known interference cancellation," *IEEE J. Sel. Areas Commun.*, vol. 21, no. 5, pp. 802–811, Jun. 2003.

[17] J. H. Winters, J. Salz, and R. D. Gitlin, "The impact of antenna diversity on the capacity of wireless communication systems," *IEEE Trans. Commun.*, vol. 42, no. 2/3/4, pp. 1740–1751, Feb./Mar./Apr. 1994.

[18] W. Yu and J. M. Cioffi, "Trellis precoding for the broadcast channel," in *Proc. Globecom*, San Antonio, TX, Nov. 2001, pp. 1344–1348.

[19] ——, "Sum capacity of a Gaussian broadcast channel," in *Proc. IEEE Int. Symp. Inf. Theory*, Lausanne, Switzerland, Jul. 2002.

[20] R. Zamir, S. Shamai (Shitz), and U. Erez, "Nested linear/lattice codes for structured multiterminal binning," *IEEE Trans. Inf. Theory*, vol. 48, no. 6, pp. 1250–1276, Jun. 2002.

Goran Dimić (M'05) received the Diploma in electrical engineering from the University of Belgrade, Belgrade, Serbia and Montenegro, and the M.S. and Ph.D. degrees in electrical engineering from the University of Minnesota, Minneapolis, in 1999, 2001, and 2004, respectively.

His research interests are in the area of signal processing for communications and networking.

Nicholas D. Sidiropoulos (M'92–SM'99) received the Diploma in electrical engineering from the Aristotelian University of Thessaloniki, Thessaloniki, Greece, and the M.S. and Ph.D. degrees in electrical engineering from the University of Maryland, College Park (UMCP), in 1988, 1990 and 1992, respectively.

From 1988 to 1992, he was a Fulbright Fellow and a Research Assistant at the Institute for Systems Research (ISR), UMCP. From September 1992 to June 1994, he served his military service as a Lecturer in the Hellenic Air Force Academy. From October 1993 to June 1994, he also was a member of the technical staff, Systems Integration Division, G-Systems Ltd., Athens, Greece. He was a Postdoctoral Fellow (1994 to 1995) and Research Scientist (1996 to 1997) at ISR-UMCP, an Assistant Professor with the Department of Electrical Engineering, University of Virginia, Charlottesville, from 1997 to 1999, and an Associate Professor with the Department of Electrical and Computer Engineering, University of Minnesota, Minneapolis, from 2000 to 2002. He is currently a Professor with the Telecommunications Division of the Department of Electronic and Computer Engineering, Technical University of Crete, Chania, Crete, Greece, and Adjunct Professor at the University of Minnesota. His current research interests are primarily in signal processing for communications, and multi-way analysis. He is an active consultant for industry in the areas of frequency hopping systems and signal processing for xDSL modems.

Dr. Sidiropoulos is a member of both the Signal Processing for Communications (SPCOM) and Sensor Array and Multichannel Signal Processing (SAM) Technical Committees of the IEEE Signal Processing Society and currently serves as an Associate Editor for the IEEE TRANSACTIONS ON SIGNAL PROCESSING. From 2000 to 2002, he also served as Associate Editor for the IEEE SIGNAL PROCESSING LETTERS. He received the NSF/CAREER award (Signal Processing Systems Program) in June 1998 and an IEEE Signal Processing Society Best Paper Award in 2001.